Conformational Changes Combined with Charge-Transfer Interactions Are Essential for Reduction in Catalysis by *p*-Hydroxybenzoate Hydroxylase†

Mariliz Ortiz-Maldonado, Barrie Entsch, and David P. Ballou*

Department of Biological Chemistry, University of Michigan, Ann Arbor, Michigan 48109-0606

Received May 6, 2003; Revised Manuscript Received July 18, 2003

ABSTRACT: *p*-Hydroxybenzoate hydroxylase is a flavoprotein monooxygenase that catalyzes a reaction in two parts: reduction of the enzyme cofactor FAD by NADPH in response to binding *p*-hydroxybenzoate to the enzyme and reaction of reduced FAD with oxygen to form a hydroperoxide, which then oxygenates *p*-hydroxybenzoate. Three different reactions, each with specific requirements, are achieved by moving the position of the isoalloxazine ring in the protein structure. In this paper, we examine the operation of protein conformational changes and the significance of charge-transfer absorption bands associated with the reduction of FAD by NADPH when the substrate analogue, 5-hydroxypicolinate, is bound to the enzyme. It was discovered that the enzyme with picolinate bound was reduced at a rate similar to that with *p*-hydroxybenzoate bound at high pH. However, there was a large effect of pH upon the rate of reduction in the presence of picolinate with a pK_a of 7.4, identical to the pK_a of picolinate bound to the enzyme. The intensity of charge-transfer bands observed between FAD and NADPH during the reduction process correlated with the rate of flavin reduction. We conclude that high rates of reduction of the enzyme require (a) the isoalloxazine of the flavin be held by the protein in a solvent-exposed position and (b) the movement of a loop of protein so that the pyridine ring of NADPH can move into position to form a complex with the isoalloxazine that is competent for hydride transfer and that is indicated by a strong charge-transfer interaction.

p-Hydroxybenzoate hydroxylase (PHBH)[1] from *Pseudomonas aeruginosa* and *Pseudomonas fluorescens* (EC 1.14.13.2) has been used extensively as a model for the reactions catalyzed by flavoprotein monooxygenases, particularly for enzymes that oxygenate aromatic compounds (*1*, *2*). The catalytic scheme for the reaction catalyzed by PHBH shown in Figure 1 is typical of this group of enzymes. In the reaction, an atom of oxygen is inserted into the aromatic ring of the substrate, and this is an important step in one of the metabolic pathways for the degradation of aromatic compounds by microorganisms. PHBH and probably many other enzymes of this type utilize a novel mechanism to link two rather different catalytic processes, the reduction of the flavin, followed by its reaction with oxygen to bring about hydroxylation of the substrate. The flavin is mobile in the enzyme. Rotation of the ribityl chain causes the isoalloxazine ring to move from an "in" position to an "out" position some 7−8 Å apart in the plane of the isoalloxazine ring (ref *3* and references cited therein). Before NADPH can reduce the flavin (by coming in contact with it), the isoalloxazine of the FAD must move to the out position (see Figure 2), and this movement requires *p*-hydroxybenzoate (pOHB) to be bound to the enzyme. With the flavin in the out position NADPH reduces the flavin. The substrate pOHB increases the rate of reduction by more than 10^5-fold. Then, after it is reduced, the isoalloxazine swings back to the in conformation of the active site, where the reduced flavin reacts with oxygen to initiate the second half of the catalysis: oxygenation of the substrate. This effectively gives PHBH two active sites to carry out two diverse reactions. Our understanding of the complexity of the function of this protein has been enhanced by a structure of NADPH bound to the mutant form of the enzyme, Arg220Gln (*4*). PHBH exhibits a motif for binding NADPH that has not been previously recognized. NADPH binds with its adenine ring next to the isoalloxazine ring of FAD and the rest of the molecule in an extended conformation with the nicotinamide ring remote from the isoalloxazine ring. The structure shows that reduction can only happen with the flavin out and with a rotation of the nicotinamide ring portion of bound NADPH to bring it within 4 Å of the isoalloxazine ring. Structural modeling suggests that a loop of protein from residue 263 to residue 271 has to move to allow rotation of the nicotinamide (*4*). This model suggests that effective reduction involves two protein changes: movement of the flavin out and movement of the loop to allow the nicotinamide of NADPH to swing into place for transfer of its hydride.

Charge-transfer (CT) interactions have been observed between flavin cofactors and substrates in many enzyme active sites [as reviewed in 1974 by Massey and Ghisla (*5*)]. When a CT interaction occurs, a new (usually broad) absorption band is observed at wavelengths longer than the

† Financial support was received from the U.S. Public Health Service (Grant GM 64711 to D.P.B.) and the Australian Research Council (A 09906323 to B.E.).

* To whom correspondence should be addressed. E-mail: dballou@umich.edu. Fax: (734) 763-4581. Phone: (734) 764-9582.

[1] Abbreviations: PHBH, *p*-hydroxybenzoate hydroxylase; pOHB, 4-hydroxybenzoate; PICO, 5-hydroxypicolinate; CT, charge transfer; 2,4-DOHB, 2,4-dihydroxybenzoate.

10.1021/bi030114y CCC: $25.00
Published on Web 09/05/2003

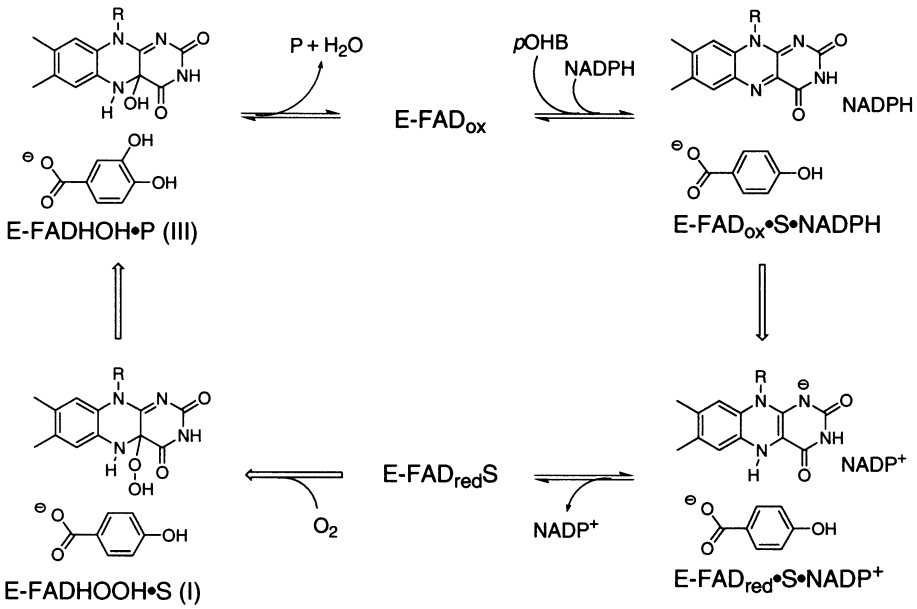

FIGURE 1: Catalytic cycle of PHBH. In the figure, E represents the enzyme, S represents pOHB, and P represents 3,4-dihydroxybenzoate, the oxygenated product.

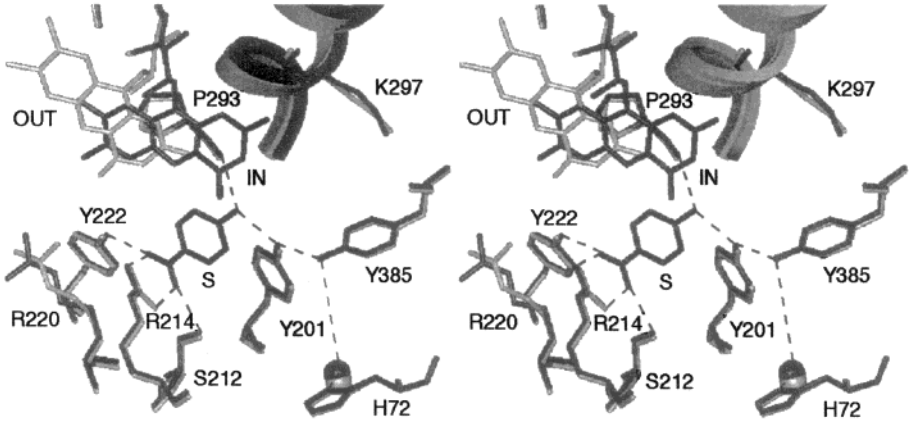

FIGURE 2: Stereoview of the active site of wild-type PHBH as the complex with pOHB (black shading, the "in" conformation), compared to the structure of the active site as the complex with 2,4-DOHB (gray shading, the "out" conformation) (*25*). Note that 2,4-DOHB is not shown. The dashed lines indicate the key residues in the proton network from the substrate phenol to the surface of the protein.

absorption bands of the participants in the interaction (*5*). An important type of CT interaction occurs in the formation of complexes between pyridine nucleotides and flavoproteins (*6*, *7*). With some flavoproteins, these charge-transfer interactions have been shown to be part of the catalytic reaction pathway (*8*, *9*) when the flavin is reduced by pyridine nucleotide. Blankenhorn (*6*) stated, "It is not clear whether the CT interaction in the complexes is merely "accidental" and unrelated to the mechanism of hydrogen transfer or whether the CT interaction is functionally significant for transfer of oxidation−reduction equivalents." Quantum chemical calculations of redox reactions between flavin and pyridine nucleotide (*10*) have shown that the process of hydride transfer between the molecules occurs when there is orbital overlap between the N-5 of the flavin and the C-4 of the pyridine ring at a distance of $\leq$2.7 Å. Recent studies with DNA (*11*) have established the importance of CT interactions in the transfer of electrons through the double helix of DNA in electrochemical processes. CT interactions in PHBH are observed between the flavin and pyridine nucleotide substrate during flavin reduction (*12*). First, CT occurs between NADPH and FAD, and then, after hydride transfer, a second CT occurs between $FADH^-$ and NADP. Under optimum conditions for PHBH, the rate of flavin reduction by NADPH in the enzyme in complex with pOHB at 25 °C is $\geq$250 s^{-1} (unpublished observation) and is thus similar to that recorded for maximum rates of reduction (345 s^{-1}) in an intramolecular model system that optimizes the orientation between free flavin and pyridine nucleotide (*6*). We have identified experimental conditions in the study of PHBH that help to clarify the role of CT interactions in reduction of this enzyme by employing the substrate analogue, 5-hydroxypicolinate (PICO; see Figure 3). This compound was found to stimulate high rates of NADPH consumption by PHBH without the formation of an oxygenated product of PICO (*13*); thus, the second product was H_2O_2, and the reaction was uncoupled from normal hydroxylation. We have found that the rate of reduction of the flavin in the presence of PICO is very dependent upon pH in the range of 6−9.5, where the protein is stable. This observation has provided us with the opportunity to examine the relationship between CT formation and the rate of reduction, which we know depends on the correct conformational state of PHBH (*3*).

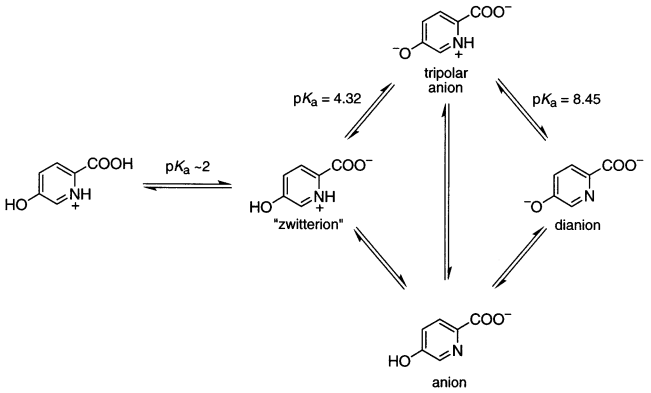

FIGURE 3: Ionization states of PICO in aqueous solution. Chemical structures and corresponding macro pK_a values determined are shown.

This paper reports an analysis of the reduction of PHBH when PICO replaces the natural substrate, pOHB. The results provide new insights into the roles of the conformational changes in PHBH for optimum flavin reduction and of CT interactions in catalysis. A preliminary report on this work was presented to the International Flavin Symposium in Konstanz (*14*).

MATERIALS AND METHODS

All common reagents used in this work were analytical reagent grade. NADPH used was at least 98% pure (from either Roche Biochemicals or Sigma). The substrate analogue, PICO, was synthesized according to the method described by Duesel and Scudi (*15*). Other substrates for PHBH were from commercial sources and were recrystallized before use.

The construction of plasmids and the methods for expression of PHBH in *Escherichia coli* have been described previously (*16*−*18*). The enzyme and mutant forms were purified as described in refs *17* and *19*. The mutant forms of PHBH (His72Asn and Arg220Lys) have been described before (*3*, *20*).

All experimental measurements with PHBH were carried out at 3−4 °C to make the reactions slow enough for quantitative analysis. The methods used were similar to those described by Moran et al. (*21*). Of particular importance were the buffers used for setting pH values with PHBH because this enzyme is inhibited by some monovalent anions. For the pH range of 6.2−7.5, potassium phosphate solutions were used; for the pH range of 7.5−8.8, Tris−sulfate was used; for the pH range 8.8−9.5, glycine adjusted with NaOH or KOH was used. No differential buffer effect was found on enzyme processes when these buffers were used.

Rapid reaction kinetic traces were analyzed and simulated with the software called Program A, an MS-DOS based series of programs developed in our laboratory by Rong Chang, Chung-Jin Chiu, Joel Dinverno, and David Ballou, University of Michigan. Analysis of reaction traces is based upon the Marquardt algorithm for fitting data to sums of exponentials (*22*).

RESULTS

5-Hydroxypicolinate. PICO is a structural analogue of pOHB, the natural substrate of PHBH (Figure 3). The important difference from pOHB is the presence of the aromatic ring nitrogen. PICO has a potentially complex array of ionic forms in aqueous solution (Figure 3), and depending upon pH, four species of PICO are observed in water. In Figure 4A, the spectra of three dominant species at pH 2.2, 6.6, and 11.3 are shown. The fourth species, observed at very low pH is not shown; it has a spectrum similar to the pH 2.2 species. In water, the species labeled "anion" in Figure 3 is a negligibly small fraction of the PICO present. This was demonstrated by taking a solution of PICO buffered at pH 6.5 and adjusting the solvent composition with dioxane [an aprotic solvent that lowers the dielectric constant of the solution (*23*, *24*)]. The principal effect of dioxane was the suppression of the peak between 300 and 350 nm (see Figure 4B). Low and high pH also suppressed the peak between 300 and 350 nm (Figure 4A). Thus, we conclude that the 325 nm peak is primarily due to the tripolar species and that the spectrum in water at pH 6.6 (Figure 4A) is dominated by the tripolar species. We do not know the exact ratio of tripolar to anion species in water. In this work, experimental measurements were made with PHBH in the pH range of 6.0−9.5, the pH range in which the enzyme is stable. Thus, the enzyme was exposed to PICO in solution that is mostly a mixture of tripolar and dianion species (Figure 3).

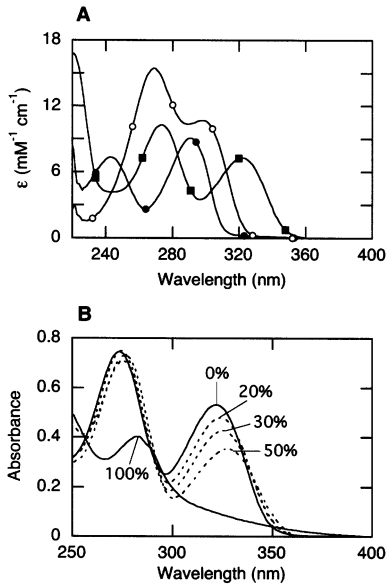

FIGURE 4: Absorption spectra of PICO with pH and in mixtures of water and dioxane. (A) Absorption spectra of PICO at pH 2.2 (● is the zwitterion), at pH 6.6 (■ is the tripolar anion), and at pH 11.3 (○ is the dianion). (B) Spectra of 72 μM PICO were recorded in the percent dioxane shown on the figure. Each solution contained 50 mM phosphate as the K salt, initially at pH 6.6. Some turbidity developed with increasing dioxane. It is clear that the absorption band of PICO at 320 nm is suppressed by dioxane.

PICO Complex with PHBH. The interaction of PICO with the resting (oxidized) enzyme was studied by following the change in the flavin spectrum as PICO was bound by PHBH next to the flavin. From pH 6.0 to pH 9.5, the result was always the same, as illustrated in Figure 5. When PICO was bound in the active site of PHBH, there was a large increase in the extinction of the FAD at 450 nm (of ~2000 M^{-1} cm^{-1}). The difference spectrum for PICO bound compared to free enzyme between 350 and 500 nm (due to FAD only; see Figure 5B) was consistent with that found when FAD in the active site takes up the out conformation (Figure 2 and ref *25*). This is in contrast to the enzyme with pOHB bound,

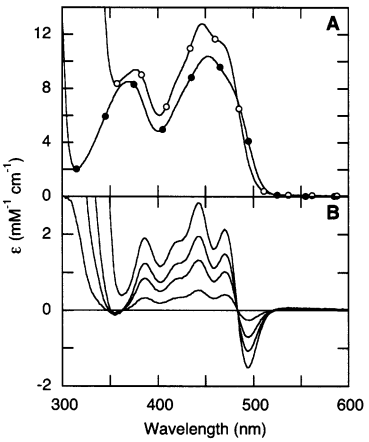

FIGURE 5: Perturbations of absorption spectra of PHBH upon binding PICO. (A) Spectra of PHBH without substrate (●) and PHBH saturated with PICO (○) in 100 mM Tris−sulfate (pH 8.65). (B) Difference spectra for the changes in (A) upon addition of 10, 30, 60, and 424 μM PICO. Note that the spectra in (A) and (B) include a contribution from PICO below 370 nm.

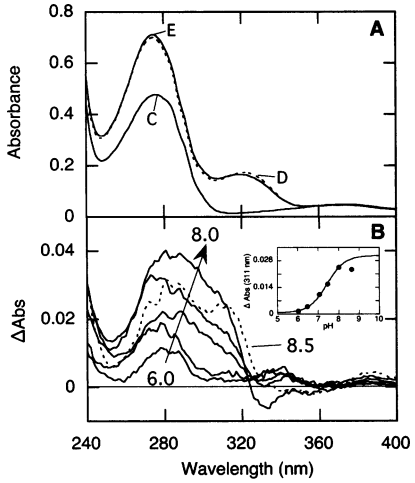

FIGURE 6: Analysis of the spectral changes resulting from binding of PICO to PHBH over a range of pH. (A) Example of information collected in a double sector cuvette: spectrum C was 5.8 μM PHBH in 50 mM phosphate as the K salt, pH 7.0, in sector 1 with the same buffer in sector 2; spectrum D (dashed line) was PHBH in sector 1 with 25 μM PICO (both in the same buffer) in sector 2; and spectrum E (solid line) was obtained after the PHBH and PICO sectors were mixed. (B) Plots of difference spectra between D and E in panel A at pH 6.02, 6.50, 7.06, 7.47, 8.0, and 8.64. These difference spectra were corrected for the fraction of unbound PICO at each pH, based upon the K_d values determined at each pH. Inset: Plot of difference spectral changes against pH. The data were fitted with a function for a pH-dependent process with a pK_a of 7.4 (solid line).

where the FAD takes up the in conformation (Figure 2 and ref *25*) when the phenol is protonated. In the crystal structure of PHBH with the flavin out (*25*), the substrate analogue, 2,4-dihydroxybenzoate (2,4-DOHB), was bound instead of pOHB. The structure shows that the 2-hydroxyl of the substrate provides a new H-bond to the N-3 position of the isoalloxazine ring that probably helps to stabilize the out conformation. When PICO replaces pOHB in the enzyme, the ring nitrogen could provide an alternative basis for a new H-bond to stabilize the out conformation. If a water molecule were positioned to H-bond to the ring N of PICO, it then could bridge to the N-3 of the isoalloxazine ring in the out conformation. This is a proposal without any direct crystallographic information.

The dissociation constant values obtained for PICO binding to PHBH (between 50 and 100 μM depending on pH) were 5−10-fold higher than those for pOHB bound to the enzyme under similar conditions. This observation suggested to us that the enzyme might prefer not to bind to the dominant tripolar species in solution (Figure 3). The natural substrate (pOHB) is known to bind to the enzyme as either the monoanion or dianion (*16*), analogous to the anion and dianion species of PICO (see Figure 3). The pK_a of the phenol of pOHB is shifted to lower pH (from 9.3 to 7.4) when bound in the enzyme active site (*16*). To determine the ionic state of PICO in the active site, a series of titrations were carried out at about 6 μM PHBH, and the spectral changes to PICO were followed as it bound to the active site over a range of pH values. Very careful measurements were carried out in a Yankeloff double-sectored spectrophotometer cell (Figure 6A). First, the spectrum of the enzyme in sector 1 with buffer in sector 2 was recorded. Second, the spectrum of the enzyme in sector 1 with the desired amount of PICO in sector 2 was recorded. Thus, we know the exact concentration of PICO to be mixed with enzyme in each experiment. Third, both sectors were mixed and the spectrum was recorded. The spectral differences obtained upon a fraction of PICO binding to PHBH had to be corrected for the calculated fraction of PICO unbound at each pH (Figure 6B). This was necessary because of the magnitude of the K_d values for PICO with the enzyme and the high extinction of PICO in solution. There was a clear trend of the absorbance differences with pH (Figure 6B, inset, where ΔA at 311 nm is plotted). The differences could be fitted to a pK_a for PICO in the active site of PHBH of 7.4, compared to the value in free solution of 8.45 (Figure 3).

Scheme 1

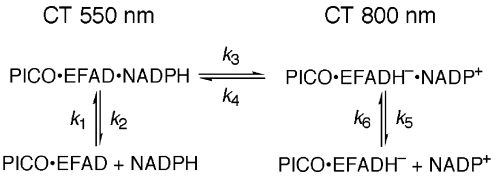

Reduction by NADPH of the FAD in the PICO Complex with PHBH. To study the reduction phase of the catalytic cycle of PHBH (Figure 1), experiments were conducted under anaerobic conditions in a stopped-flow spectrophotometer at 3−4 °C. This temperature was necessary to slow the reactions sufficiently to resolve intermediates. Solutions of PHBH in complex with PICO were mixed with solutions of NADPH to initiate the reduction of the enzyme flavin by NADPH (PICO replaces pOHB in Figure 1), followed by the release of NADP formed. In these experiments PHBH is saturated with PICO (based on the measured K_d values determined separately). Thus, the reaction measured was the reduction reaction shown in Scheme 1. To analyze this reaction, absorbance changes were followed in the range of 420−825 nm. In this range of wavelengths, absorbance is due only to contributions from FAD (420−520 nm) and any CT bands formed between flavin and pyridine nucleotide (520−825 nm). This was established first by Howell et al. in 1972 (*12*) for the reaction with the natural substrate, pOHB. In the reactions with PICO, small absorbance changes extend even beyond 825 nm but could not be followed due

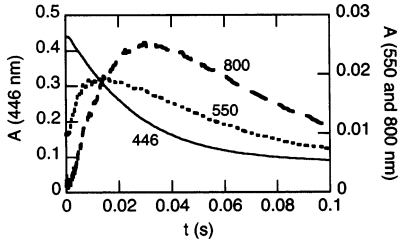

FIGURE 7: Reaction traces obtained by absorbance for the reduction of the complex between PHBH and PICO with NADPH. The reaction solution after being mixed in the stopped-flow spectrophotometer contained 34 μM PHBH, 4 mM PICO, 4.8 mM NADPH, and 50 mM glycine (adjusted with KOH) at pH 9.4 and 3 °C. Absorbance changes are shown for 446 nm (solid line), 550 nm (dotted line), and 800 nm (dashed line).

to limitations of the instrumentation. Absorbance changes measured showed that CT interactions were occurring during the reduction reactions. Examples of absorbance changes are shown in Figure 7 for reactions at pH 9.4 and 3.0 °C. At 446 nm, the reaction is dominated by a large decrease in absorbance due to the reduction of FAD. However, absorbance changes at 446 nm require three exponentials to fit the changes; in addition to the reduction, there is a fast, initial process causing a small lag that varies in rate with NADPH concentration (first step in Scheme 1, ~250 s^{-1} at 5 mM NADPH) and a slower final small decrease in absorbance that corresponds to the final change measured at 800 nm (last step in Scheme 1). At 550 nm, the small absorbance change is due principally to CT interaction between oxidized FAD and NADPH, since there is an increase in absorbance that is partly complete within the dead time of the instrument (1.5 ms for the experiment shown in Figure 7), followed by a biphasic decrease in absorbance that is dominated by a change at the same rate as reduction monitored at 446 nm. By contrast, at 800 nm (Figure 7), the absorbance change must be due to principally the CT interaction between $FADH^-$ and NADP. Thus, there is an increase in absorbance that corresponds in rate to the reduction of FAD at 446 nm ($k_{3,obs}$ of 48 ± 2 s^{-1}), which is followed by a decrease in absorbance that is slightly slower than that of reduction ($k_{5,obs}$ of 40 ± 5 s^{-1}), corresponding to dissociation of NADP. These small absorbance changes were analyzed more accurately by taking multiple shots and averaging the results. Enzyme concentrations were high enough to ensure that the long-wavelength changes could be measured. In summary, the results at all wavelengths examined were fitted by the same three measured rate constants (corresponding to the three steps in Scheme 1).

The difference between the standard redox potentials at pH 7 for NADPH and ligand-bound PHBH is approximately 160 mV. When this difference is combined with reaction conditions where the ratio of NADPH to NADP is high, then the hydride transfer (the middle step in Scheme 1) is effectively irreversible. The ratio of k_3 to k_4 in Scheme 1 must be at least 2.5×10^5, and in practical terms, k_4 is 0. The absolute rates of reduction of FAD in the reactions at each pH (k_3) were calculated from measurements of the observed rates of reduction over a range of NADPH concentrations. An example of results at pH 9.4 is shown in Figure 8. The observed rate of reduction was obtained from the large decrease in absorbance at 446 nm after three exponential processes were fitted to the reaction traces, as

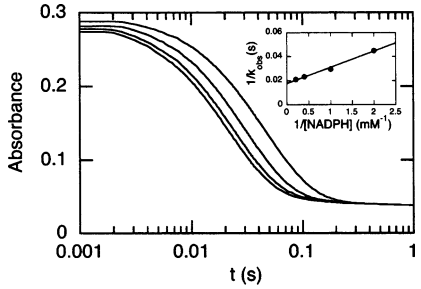

FIGURE 8: Illustration of the dependence of the observed rates of reduction of the complex between PHBH and PICO upon the concentration of NADPH. The figure shows the change in absorbance at 446 nm in reactions containing the following concentrations of NADPH: 0.5, 1.0, 2.5, and 5.0 mM. The rate of decrease in absorbance increases with increasing concentration of NADPH (note the log time scale). The experimental conditions were similar to those given in the legend to Figure 7, except that the enzyme concentration was 24 μM and the temperature 4 °C. Inset: Plot of the reciprocal of the observed rate constant against the reciprocal of NADPH concentration. From this plot, the rate of reduction of the enzyme was calculated as 54 $s^{-1}$and the K_d for the complex with NADPH as 0.70 mM.

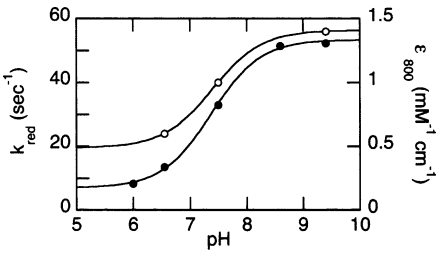

FIGURE 9: Comparison between the dependence of the rate of reduction of the complex of PHBH and PICO and of the calculated extinction of the CT band at 800 nm upon pH. The rate constants (●) were obtained from extrapolations to infinite NADPH concentration as illustrated in Figure 8. The intrinsic extinction values at each pH (○) were calculated as described in Results. Each extinction represents the average of the complexes in the protonated and the unprotonated forms. The solid lines represent fits to a single process with a pK_a of 7.4. The limiting values for rates were 6.9 and 54 s^{-1} and for extinctions, 0.49 and 1.4 mM^{-1} cm^{-1}.

discussed in the paragraph above and shown in Scheme 1. By abstracting out the reduction process, the analysis of Scheme 1 was simplified to a two-step process. A double reciprocal plot of the observed rate of FAD reduction versus NADPH concentration gave a straight line in all experiments (see Figure 8 inset). On the basis of the kinetic analysis described by Strickland et al. (*26*), the intercept on the reciprocal rate axis is the reciprocal of the reduction rate constant (k_3). The slope divided by the intercept in these reciprocal plots provides a measure of K_d (or the ratio of k_2 to k_1 in Scheme 1). The final pH of each reaction was measured on the mixed solutions from the stopped-flow experiments. The calculated rate constants for reduction at each pH are plotted against pH (Figure 9). The reduction rate constant at pH 9.4 (54 s^{-1}) was only slightly less than that for PHBH reduction with pOHB bound under the same conditions (74 s^{-1}) (*3*). At pH 6.0, the rate of reduction was nearly 8-fold slower, unlike with pOHB bound, which is only 2-fold slower than at pH 9.4. This significant pH dependence was fitted to a theoretical curve for a single pK_a of 7.4 (Figure 9); the fit was excellent.

CT Band Changes with pH. We also measured the intensity of observed CT bands at different pH values to see if these

Table 1: Parameters Used in the Simulation of Reaction Traces at 800 nm To Obtain CT Band Extinctions[a]

parameter[b]	pH 6.5	pH 7.5	pH 9.4
NADPH (mM)	1.82	2.5	5.0
PICO·EFAD (mM)	0.0285	0.0255	0.0245
k_1 (M^{-1} s^{-1})	5×10^4	5×10^4	5×10^4
k_2 (s^{-1})	12	19	24
k_3 (s^{-1})	12	33	50
k_5 (s^{-1})	40	40	40

[a] At 800 nm, there is no extinction for components other than PICO·EFAD·NADPH and PICO·EFADH$^-$·NADP$^+$. The values for the oxidized CT complex were small compared to the reduced CT complex, as shown by the ~0 absorbance at the start of the trace at 800 nm (Figure 7). Values for rate constants k_4 and k_6 were set at zero as explained in the Results. [b] As shown in Scheme 1.

intensities correlated with rates of reduction. The CT interaction between FAD and NADPH could not be analyzed accurately, because of small absorbance changes and high rates. The complex between PHBH and NADPH was formed reversibly at rates of hundreds per second (at 3.5 °C as can be seen in Figure 7, 550 nm trace; the observed rate of the first phase is in the range of 250−350 s^{-1}), and the CT band had a very low absorbance and could not be distinguished spectrally from the subsequent CT interaction between FADH$^-$ and NADP at any wavelength examined. However, the complex between FADH$^-$ and NADP was formed at the rate of flavin reduction, had a measurable absorbance, and was the dominant species absorbing at 800 nm. Thus, traces at 800 nm (as in Figure 7) provided a reasonable signal to analyze the changes in CT interactions at different pH values. The most important CT interaction for directing the proper orientation for reduction is the one between FAD and NADPH, but this CT complex is too difficult to quantify. However, it is reasonable to assume that the CT interaction between FADH$^-$ and NADP is also a reporter on reduction because it is the immediate product of the hydride transfer from the first CT complex. It is also an essential intermediate in catalysis by PHBH (*29*) and is partially formed when a high concentration of NADP is added to reduced enzyme in complex with pOHB (unpublished results). Thus, the complex is on the pathway for the reversal of reduction. The analysis was simplified when it was found that the dissociation of NADP from the enzyme occurred with the same rate constant at all pH values studied (40 s^{-1}). This was shown by the measurement of a constant exponential of 40 s^{-1} in the formation and decay of the absorbance at 800 nm. Thus, the rate of formation of the CT interaction between FADH$^-$ and NADP (equivalent to reduction) varied with pH (Figure 9), but the CT decomposed at the same rate (40 s^{-1}). Because these two rates are very similar in value, the observed absorbance maxima at 800 nm never approach full formation of the potential CT interaction. Thus, it was only possible to obtain the extinction of the CT interaction by simulating the full reaction in Scheme 1 at each pH.

Three pH values that spanned the observed pK_a in reduction of the complex between PHBH and PICO (Figure 9) were chosen for simulation. At each pH, absorbance traces at 800 nm were recorded under identical conditions and averaged. The model described by Scheme 1 was simulated numerically with Program A, which uses the Runge−Kutta algorithm for integrating differential equations (*22*, *27*); the parameters used are shown in Table 1. The value for k_4 was essentially 0 as described above. The value for k_6 was assumed to be 0, because the reactions simulated were carried out with at least 2 mM NADPH and 0 mM NADP. At the highest the value of $k_{6,obs}$ would be less than 1% of the rate of k_5. Thus, the rate of disappearance of the absorbance at 800 nm was the value of k_5. Reaction traces were compared at concentrations of NADPH that were nearly saturating the enzyme to maximize the absorbance signal at 800 nm. The values of k_1 , k_3, and k_5 were obtained by experimental measurement as described before, and the value for k_2 was calculated from the measured K_d for NADPH and the value of k_1. At 800 nm, the only contribution to absorbance was due to the CT interaction (as described above) between FADH$^-$ and NADP$^+$. The concentrations of starting components were known; thus, the extinction of the CT band formed at 800 nm (due to the species PICO·FADH$^-$·NADP$^+$ in Scheme 1) was obtained by simulation of the experimental traces at this wavelength. The values obtained are plotted on Figure 9. The extinction of the CT band showed the same qualitative dependence on pH as the rate of reduction.

DISCUSSION

It has been shown in studies with the natural substrate, pOHB, that PHBH prevents NADPH from coming into effective contact with FAD until certain conditions are met (*3*). First, the aromatic substrate to be modified must be in the substrate-binding site. In addition, the protein must also facilitate a deprotonation of the buried phenolic group of the substrate. This occurs by means of the proton network consisting of substrate, Tyr201, Tyr385, water, and His72 (see Figure 2). Only when the phenolate form of the substrate is formed in the active site can the NADPH come into contact with the enzyme FAD to bring about rapid reduction (*3*, *28*). This is because the phenolate form of pOHB induces the conformational changes required to swing the isoalloxazine of FAD to the out position (Figure 2), where it comes into the critical reaction distance for reduction by NADPH. A rate acceleration of 10^5-fold for reduction of the flavin by NADPH occurs when PHBH binds pOHB (*29*). When the FAD is reduced, the isoalloxazine swings back to the in position for reaction with oxygen.

This paper describes what happens when PICO replaces pOHB in the active site of PHBH. First, when PICO binds to PHBH, the FAD (unlike with pOHB present) assumes the out conformation at all pH values studied, based upon the spectral changes observed (Figure 5 for pH 8.6 and ref *25*). Similar behavior is found for the WT enzyme with 2,4-DOHB bound (*25*) and for the mutant enzyme, Arg220Lys, on binding pOHB (*20*). PICO also has its phenolic group in the correct position to interact with the proton network that has been shown to promote deprotonation of the phenolic group of pOHB in the active site (see Figure 2 and refs *3* and *28*). Because the out conformation is essential for reduction of flavin by NADPH (above), it would be reasonable to predict that pH would have no effect upon reduction when PICO is bound to the enzyme. However, if reduction also requires that the phenolate stimulates more protein changes than moving the flavin out, then there should be a pH effect on reduction in the presence of PICO, and it should be sensitive to the pK_a of His72 (6.2) at the solvent end of the proton network (*3*). However, neither prediction

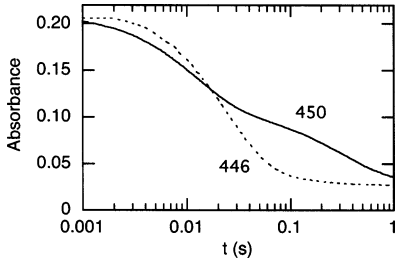

FIGURE 10: Reduction of the mutant of PHBH, His72Asn, in complexes with either PICO or pOHB. Reduction was followed by absorbance (at the wavelengths marked on the figure) in the stopped-flow spectrophotometer under anaerobic conditions. Final solutions contained His72Asn (20 μM) with pOHB (0.5 mM) or His72Asn (17 μM) with PICO (2.0 mM), NADPH (2.5 mM), and Tris−sulfate buffer (50 mM in Tris), pH 8.6 at 4 °C. The solid line is for reduction of the complex with pOHB, as published previously (*3*). Note two distinct reduction phases occur: one with a rate of ~75 s^{-1} and the other, ~3 s^{-1}. The dashed line is for reduction in the complex with PICO. This reduction occurs with a single rate of 41 s^{-1}.

is correct. Instead, reduction of PHBH in complex with PICO has a pH dependence that directly reflects the pK_a of PICO (7.4) in the active site (Figures 6 and 9). Because the measured pK_a is similar to a residue such as His72, we could not rule out His72 ionization on the basis of the experimental results. The PHBH mutant, His72Asn, disrupts the proton network and has been used to demonstrate the function of this network in PHBH (see Figure 2). With pOHB, two distinct forms of His72Asn are observed: one with pOHB as the monoanion and one with pOHB as the dianion. These distinct forms of the mutant do not interconvert rapidly (*3*, *28*), and therefore reduction of the flavin occurs in two distinct phases (Figure 10). We have found that the His72Asn mutant form with PICO does not exhibit two phases of reduction as it does with pOHB; with PICO, it behaves like WT as illustrated in Figure 10, indicating that the proton network has much less importance to reduction. Our interpretation of these observations is that, when PICO binds to PHBH, the flavin of the oxidized enzyme is in the out conformation, and there is probably a solvent connection to the substrate-binding site (*25*, *28*) that can facilitate proton exchange. Thus, the proton network of the protein (Figure 2) is not required to mobilize the phenolic proton of PICO in this conformation. The positive electrical field of the active site (*21*) probably promotes dissociation of the phenolic proton, thus lowering the observed pK_a for PICO (Figure 6B, inset).

An important conclusion from the studies with PICO concerning control of reduction in PHBH is that the out conformation is necessary, but not sufficient, for maximum rates of FAD reduction. In addition to triggering movement of the flavin out, formation of the phenolate anion of the substrate is also necessary for achieving the correct orientation of NADPH to FAD. There must be a signal transmitted through the protein structure to affect some aspect of NADPH binding. This might be achieved through repulsion (by the substrate phenolate anion) of the carbonyl of Pro293, which is within H-bonding distance from the substrate phenol (ref *30* and Figure 2). This proposal for reduction in the presence of PICO differs from the earlier proposal that the formation of the phenolate of pOHB is responsible for the formation of the out conformation when reduction occurs

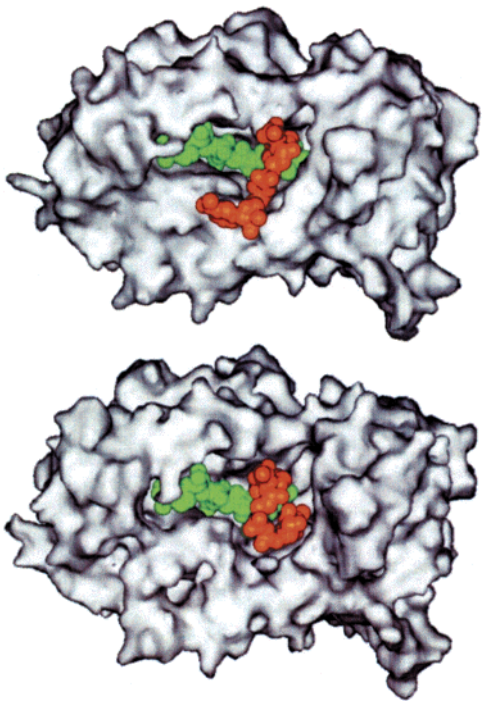

FIGURE 11: Illustration of the complex formed between PHBH and NADPH. The top picture shows a surface rendering of one subunit of the mutant Arg220Gln of PHBH (*4*) from the perspective where FAD is visible (green), but the isoalloxazine is buried in the protein on the right end of the FAD structure. NADPH (orange) is bound approximately perpendicular to the flavin, with the adenine ring buried near the *si* side of the isoalloxazine ring and the nicotinamide ring on the surface far removed from the isoalloxazine (pointing down). This structure is consistent with the fact that PHBH always binds NADPH but strictly controls hydride transfer from NADPH to FAD in response to pOHB. The bottom picture is a model of the conformation required when hydride transfer occurs after being triggered by the binding of pOHB or PICO and deprotonation of the substrate phenol in the active site. The protein strand from residue 263 to residue 271 was moved, and NADPH was rotated so that the nicotinamide can reduce the isoalloxazine in the out conformation. The structure went through energy minimizations before creation of the picture. Thus, the surface of the protein shows many subtle changes to accommodate the movements.

(*3*, *31*). In that earlier work, it was suggested that repulsion by the phenolate of the carbonyl of Pro293 causes changes in the active site loop between residues 292 and 300 that favor the out conformation when NADPH binds. With PICO, this change must occur upon substrate binding, before NADPH interacts with the enzyme. Then, with NADPH bound, the phenolate (through the repulsion of the carbonyl of Pro293) triggers another change that stimulates reduction. Presumably, with the natural substrate (pOHB) bound, formation of the phenolate initiates both movement of the isoalloxazine out and the second change that influences NADPH.

The recent solution of the structure of PHBH (as the mutant Arg220Gln) with NADPH bound (*4*) provides a ready structural explanation for the observations about reduction discussed above. This structure showed that NADPH was bound to the surface of the protein in an extended conformation, with the adenine ring of NADPH located near the *si* side of the isoalloxazine ring and the nicotinamide ring far removed from the isoalloxazine (Figure 11, top). Reduction could only happen with the flavin moved out and with the nicotinamide ring of NADPH rotated from the position

observed in the structure to lie within 3 Å of the isoalloxazine ring. Structural modeling suggested that a loop of protein from residue 263 to residue 271 should move to allow complete nicotinamide rotation to meet the isoalloxazine ring (ref *4* and Figure 11, bottom). The results presented in this paper show that two processes are required to achieve close contact between FAD and NADPH: the isoalloxazine ring must move to the out conformation, and another change must be induced by substrate ionization. It is possible that the second change is the rotation of residues 263−271 so that the nicotinamide ring can swing completely to meet the flavin ring.

If the proposal above is correct, then the mechanism of reduction of PHBH with PICO bound should also occur with the substrate analogue, 2,4-DOHB, which also forces the protein into the out conformation. We have observed the same type of dependence of reduction rate constant on pH (unrelated to the proton network) with 2,4-DOHB bound to the enzyme [pK_a of 7.8 with a rate of 24 s^{-1} at high pH and 3.5−4 °C (unpublished results) and a rate of 0.8 s^{-1} at low pH (*21*)]. Further support for our interpretation of the PICO results has come from studies of the mutant, Arg220Lys (*20*). The Arg220Lys enzyme adopts the out conformation when it binds pOHB and shifts the pK_a of the substrate phenol bound in the active site to 5.8 (rather than 7.4 for pOHB in WT). With this mutant, the rate constant for reduction of the enzyme in the presence of pOHB or PICO is independent of pH between pH 6.5 and 9.5 (unpublished results). The independence of this rate on pH must result from the substrate phenol being in the anionic form over the entire pH range under study so that the movement of the loop from residue 263 to residue 271 readily occurs.

CT interactions in the reduction phase of PHBH catalysis were reported many years ago (*12*) for reduction of WT in the presence of pOHB. CT absorption bands with an apparently lower extinction were also observed when WT enzyme was reduced in the complex with 2,4-DOHB at pH 8.0 (*32*). No connection was made between the possible extinctions of the CT bands and the different rates of reduction. There was no knowledge at that time about the structure of PHBH. With our current knowledge about the mechanism of control of reduction through conformational changes in the protein, it is clear that rates of reduction of PHBH by NADPH (which can vary by a factor of 10^5-fold) reflect the changes in conformational states and the resultant proximity of the FAD and NADPH rather than changes in the intrinsic reactivity of NADPH with FAD. This idea has been reinforced in recent work with different 8-substituted flavins in PHBH (*33*), where the rates of flavin reduction by NADPH were inversely correlated with the size and hydrophobicity of the substituent at the 8-position of the flavin (i.e., impediments to movement rather than response to redox potential). We have now shown that the rates of reduction of wild-type enzyme (Figure 9) correlate well with the intensity of CT interactions. In qualitative terms, the same relationship has been observed for reduction of PHBH with 2,4-DOHB bound. At pH 6.5, PHBH is reduced at only 0.8 s^{-1} (*21*) and no CT interactions could be detected. However, at pH 8.8, where the enzyme is reduced at 23 s^{-1} (about one-third of the optimal rate for reduction of PHBH with pOHB bound under these conditions), CT bands for both NADPH in complex with FAD and NADP in complex with $FADH^-$ are clearly observed beyond 550 nm. The observed CT band extinctions (Figure 9) must be indicative of the fraction of enzyme molecules that form the correct interaction between NADPH and FAD for reduction to occur at high rate under a particular set of conditions. Thus, we conclude that CT interactions are not incidental to a high rate of reduction of PHBH in the normal catalytic cycle. Rather, the interactions of FAD and NADPH that lead to CT interactions are also indicative of the correct proximity and orientation of the isoalloxazine and nicotinamide rings for achieving a high rate of reduction.

The clear correlation between CT interactions and optimal reduction in PHBH does not apply to some enzymes from the family of flavoprotein hydroxylases. For example, the comparable flavoprotein hydroxylase, 2-methyl-3-hydroxypyridine-5-carboxylic acid oxygenase (under conditions similar to those used to study PHBH in this paper), is reduced at 32 s^{-1}(*24*), only ∼2-fold slower than PHBH. However, there was no evidence in transient kinetic studies of formation of any CT complexes. It should be noted that the binding of both NADH and substrate occurred in several steps, suggesting conformational rearrangements in control of reduction (*24*). A more complex example is anthranilate hydroxylase, where reduction of one conformational form of the enzyme is very fast (280 s^{-1}) under the same conditions as used in this paper (*34*), yet there was no evidence found for CT complexes in reduction of this enzyme. Thus, there are examples of enzymes that show CT complexes on the catalytic pathway for flavin reduction as well as exceptions to this observation. Both possibilities appear to be consistent with the theoretical analysis of flavoprotein reduction by pyridine nucleotides (*10*). Hydride transfer between flavin and pyridine is primarily dependent upon the correct orientation and approach of the N-5 of the flavin and the C-4 of the pyridine ring of the nucleotide. In this orientation, C, H, and N are almost collinear, and the pyridine ring can partly overlay the isoalloxazine ring, which would yield CT interactions in the development of this orientation for reduction (as seen with PHBH) and in the transition state for hydride transfer (*10*). However, CT interactions might not be observed if the pyridine ring is held in a rotated position where it does not overlap the isoalloxazine ring, but the collinearity of C, H, and N is maintained for efficient hydride transfer. This may be the case with 2-methyl-3-hydroxypyridine-5-carboxylic acid oxygenase. It has also been found in model systems (*35*) that CT interactions during hydride transfer depend on the specific orientation of the pyridine ring to the isoalloxazine ring. Thus, although CT interactions are an indication of close contact between flavin and pyridine nucleotide and may indicate if the orientation for efficient hydride transfer has been achieved, CT interactions are not absolutely necessary for efficient hydride transfer.

ACKNOWLEDGMENT

The authors thank the late Vincent Massey for input into the analysis of the significance of the experiments reported, Bruce Palfey for valuable discussions about the manuscript, and Domenico Gatti for stimulating discussions and providing the illustrations for Figure 11.

REFERENCES

1. Entsch, B., and vanBerkel, W. J. H. (1995) *FASEB J. 9*, 476−483.
2. Palfey, B. A., and Massey, V. (1998) in *Comprehensive Biological Catalysis* (Sinnott, M., Ed.) Vol. III, pp 83−154, Academic Press, San Diego.
3. Palfey, B. A., Moran, G. R., Entsch, B., Ballou, D. P., and Massey, V. (1999) *Biochemistry 38*, 1153−1158.
4. Wang, J., Ortiz-Maldonado, M., Entsch, B., Massey, V., Ballou, D. P., and Gatti, D. L. (2002) *Proc. Natl. Acad. Sci. U.S.A. 99*, 608−613.
5. Massey, V., and Ghisla, S. (1974) *Ann. N.Y. Acad. Sci. 227*, 446−465.
6. Blankenhorn, G. (1976) in *Flavins and Flavoproteins* (Singer, T. P., Ed.) pp 261−267, Elsevier, Amsterdam.
7. Blankenhorn, G. (1975) *Eur. J. Biochem. 50*, 351−356.
8. Strickland, S., and Massey, V. (1973) *J. Biol. Chem. 248*, 2953−2962.
9. Schopfer, L. M., and Massey, V. (1979) *J. Biol. Chem. 254*, 10634−10643.
10. Mestres, J., Duran, M., and Bertrán, J. (1996) *Bioorg. Chem. 24*, 69−80.
11. Boon, E. M., Ceres, D. M., Drummond, T. G., Hill, M. G., and Barton, J. K. (2000) *Nat. Biotechnol. 18*, 1096−1100.
12. Howell, L. G., Spector, T., and Massey, V. (1972) *J. Biol. Chem. 247*, 4340−4350.
13. Entsch, B., Ballou, D. P., Husain, M., and Massey, V. (1976) *J. Biol. Chem. 251*, 7367−7379.
14. Entsch, B., Ortiz-Maldonado, M., and Ballou, D. P. (1999) in *Flavins and Flavoproteins 1999* (Ghisla, S., Kroneck, P., Macheroux, P., and Sund, H., Eds.) pp 391−394, Rudolf Weber, Berlin.
15. Duesel, B., and Scudi, J. V. (1949) *J. Am. Chem. Soc. 71*, 1866−1867.
16. Entsch, B., Palfey, B. A., Ballou, D. P., and Massey, V. (1991) *J. Biol. Chem. 266*, 17341−17349.
17. Palfey, B. A., Entsch, B., Ballou, D. P., and Massey, V. (1994) *Biochemistry 33*, 1545−1554.
18. Moran, G. R., and Entsch, B. (1995) *Protein Expression Purif. 6*, 164−168.
19. Entsch, B. (1990) *Methods Enzymol. 188*, 138−147.
20. Moran, G. R., Entsch, B., Palfey, B. A., and Ballou, D. P. (1996) *Biochemistry 35*, 9278−9285.
21. Moran, G. R., Entsch, B., Palfey, B. A., and Ballou, D. P. (1997) *Biochemistry 36*, 7548−7556.
22. Press, W. H., Teukolsky, S. A., Vettering, W. T., and Flannery, B. P. (1992) in *Numerical Recipes in C, The Art of Scientific Computing*, 2nd ed., pp 683−688, Cambridge University Press, New York.
23. Metzler, D. E., and Snell, E. E. (1955) *J. Am. Chem. Soc. 77*, 2431−2437.
24. Chaiyen, P., Brissette, P., Ballou, D. P., and Massey, V. (1997) *Biochemistry 36*, 13856−13864.
25. Gatti, D. L., Palfey, B. A., Lah, M. S., Entsch, B., Massey, V., Ballou, D. P., and Ludwig, M. L. (1994) *Science 266*, 110−114.
26. Strickland, S., Palmer, G., and Massey, V. (1975) *J. Biol. Chem. 250*, 4048−4052.
27. Bevington, P. R. (1969) *Data Reduction and Error Analysis for the Physical Sciences*, pp 235−242, McGraw-Hill, New York.
28. Frederick, K. K., Ballou, D. P., and Palfey, B. A. (2001) *Biochemistry 40*, 3891−3899.
29. Husain, M., and Massey, V. (1979) *J. Biol. Chem. 254*, 6657−6666.
30. Gatti, D. L., Entsch, B., Ballou, D. P., and Ludwig, M. L. (1996) *Biochemistry 35*, 567−578.
31. Palfey, B. A., Basu, R., Frederick, K. K., Entsch, B., and Ballou, D. P. (2002) *Biochemistry 41*, 8438−8446.
32. Spector, T., and Massey, V. (1972) *J. Biol. Chem. 247*, 5632−5636.
33. Ortiz-Maldonado, M., Gatti, D. L., Ballou, D. P., and Massey, V. (1999) *Biochemistry 38*, 16636−16647.
34. Powlowski, J., Ballou, D., and Massey, V. (1989) *J. Biol. Chem. 264*, 16008−16016.
35. Palfey, B. A., and Hu, Y.-C. (2002) *in Flavins and Flavoproteins 2002* (Chapman, S. K., Perham, R. N., and Scrutton, N. S., Eds.) pp 317−322, Rudolf Weber, Berlin.

BI030114Y